A partitioning methodology of complex uncertain structural-acoustic systems in the low and medium frequency ranges

L. Gagliardini, M. Kassem, Christian Soize

A partitioning methodology of complex uncertain structural-acoustic systems in the low and medium frequency ranges

Gagliardini L.[(1)] , Kassem M.[(1,2)], Soize C.[(2)]
[(1)] PSA Peugeot-Citroën, Industrial and Technical Division
Route de Gisy, 78 VELIZY-VILLACOUBLAY
[(2)]Université Paris-Est, Laboratoire de Modélisation et Simulation Multi Echelle,
MSME UMR 8208 CNRS, 5 Bd Descartes,77454 Marne-la-Vallee, France

Abstract
In this paper a structural zone partitioning methodology of complex uncertain structural-acoustic systems is presented. This methodology is based on an energy-field formulation of the vibroacoustic problem. In this energy-field formulation, the vibroacoustic system is modelled using statistical averaging over independent realizations of a probabilistic vibroacoustic model. In the vibroacoustic energy model, excitations are represented in terms of input power, observations are represented in terms of response power, and the propagation between excitation and observation points is represented by a set of Power Frequency Response Functions (PFRF).When statistically averaged, these parameters are linearly related to form the equation of the vibroacoustic energy model. It is shown that above a given frequency the power frequency response functions are much less dependant, on the direction or on the precise location of the excitation or the observation, than the classical frequency response functions. Consequently, a simplified model can be constructed based on a scalar frequency response function. A methodology, which consists in finding a structural partitioning of the complex system for which this simplified model is valid, is developed. Partitioning criteria are thus introduced in order to evaluate simultaneously, the error associated to the model simplification and the pertinence of a given zone partitioning. An application of this partitioning methodology to an automotive vehicle structure is presented.

1 Introduction

Uncertainty issues are of major interest in industrial vibroacoustic studies, due to the high dynamic sensitivity to small systems changes. As an example, fig.1 shows measurements of structural Frequency Response Functions (FRF) performed on 40 production vehicles, considered identical regarding vibroacoustic design.

Changes that cause the observed spread may result from process uncertainties (mainly geometrical uncertainties at various scales and their consequences in terms of stiffness, internal stress or material behaviour…) or from product diversity (product contents). When considering the overall design process, it should be mentioned that the changes in the design itself -that occurs continuously during the design phase- may also generates a variability of at least the same order of magnitude. Although the nature of those changes is very different –the first related to mechanical facts, the second to more conceptual facts-, they cause a spread of actual responses when compared to a unique design model. By the way, the use of a model is by itself a factor of uncertainty.

Recent work [1-2] showed that it is possible to globally model every kind of uncertainties, by using a probabilistic modelling, involving random matrices and based upon a maximum of entropy principle. Such a modelling ensures any physical change, within a given range, to be accounted for whatever its nature. The range of variation is controlled by the so-called dispersion parameters. These parameters are related to

the variances of the mechanical operators of the structural-acoustic problem: mass, stiffness and damping. This theory was successfully applied to large size structural-acoustic problems such as the ones encountered in the automotive industry [3], providing new tools to investigate uncertain dynamic systems, and more especially the ones with a high dynamic sensitivity.

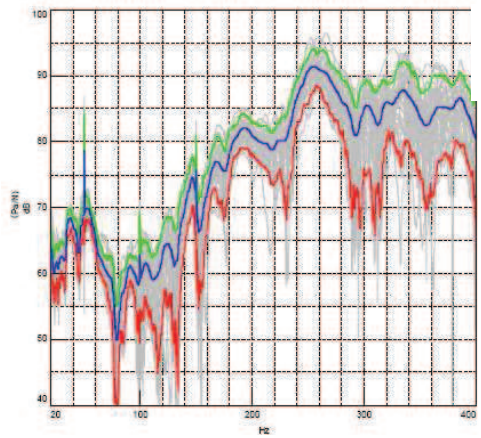

Figure 1: Vibroacoustic frequency response functions measured between the driver's ear position and a point on the body framework for 40 production vehicle (gray). Statistical average (blue), 5th centile (red) and 95th centile (green)

After a short overview of the probabilistic modelling process, an energy field approach is proposed which exhibit interesting averaged properties for uncertain systems. Applications are performed on current industrial models of vehicles, involving about 10^6 Degrees Of Freedom (DOF).

2 Stochastic modelling for vibro-acoustic problems

Probabilistic models described in this section are precisely described in [3]. The method used is a non-parametric probabilistic method, since its probabilistic aspects are not related to any of the system parameters.

For automobile problems, although source terms may also be uncertain, they are generally less dispersed than the car body FRFs. In the following, source terms will be kept constant.

2.1 Stochastic structural-acoustic problem setting and solving

We name here a "mean model" the deterministic model upon which the stochastic model is based. The mean model is such as its mechanical operators are equal to the mean mechanical operators of the stochastic model.

Classically [4], structural-acoustic problems are solved using Finite Elements Methods and a frequency domain solution. Mechanical equations in continuous media then lead to a matrix form such as:

$$\begin{bmatrix} \underline{\mathbf{A}}^{s}_{n_s}(\omega) & \underline{\mathbf{C}}_{n_s,n_a} \\ \omega^2 \underline{\mathbf{C}}^{T}_{n_s,n_a} & \underline{\mathbf{A}}^{a}_{n_a}(\omega) \end{bmatrix} \begin{bmatrix} \underline{\mathbf{u}}^{s}(\omega) \\ \underline{\mathbf{p}}^{a}(\omega) \end{bmatrix} = \begin{bmatrix} \underline{\mathbf{f}}^{s}(\omega) \\ \underline{\mathbf{Q}}^{a}(\omega) \end{bmatrix} \quad (1)$$

where $\underline{\mathbf{u}}^{s}$ (resp. $\underline{\mathbf{p}}^{a}$) is the vector of complex amplitudes of the structural (resp. acoustic) response at the nodes locations (physical coordinates) to the excitations represented by vectors $\underline{\mathbf{f}}^{s}(\omega)$ and $\underline{\mathbf{Q}}^{a}(\omega)$; $\underline{\mathbf{A}}^{s}_{n_s}(\omega)$ is the *in vacuo* dynamic stiffness matrix, such that

$\underline{\mathbf{A}}^{s}_{\mathbf{n}_s}(\omega) = -\omega^2 \underline{\mathbf{M}}^{s}_{\mathbf{n}_s} + j\omega \underline{\mathbf{D}}^{s}_{\mathbf{n}_s} + \underline{\mathbf{K}}^{s}_{\mathbf{n}_s}$ where $\underline{\mathbf{M}}^{s}_{\mathbf{n}_s}, \underline{\mathbf{D}}^{s}_{\mathbf{n}_s}, \underline{\mathbf{K}}^{s}_{\mathbf{n}_s}$ are respectively the structural mass, damping and stiffness matrices, $\underline{\mathbf{A}}^{a}_{\mathbf{n}_a}(\omega)$ is the cavity –with blocked boundary- admittance matrix, such that, $\underline{\mathbf{A}}^{a}_{\mathbf{n}_a}(\omega) = -\omega^2 \underline{\mathbf{M}}^{a}_{\mathbf{n}_a} + j\omega \underline{\mathbf{D}}^{a}_{\mathbf{n}_a} + \underline{\mathbf{K}}^{a}_{\mathbf{n}_a}$ where $\underline{\mathbf{M}}^{a}_{\mathbf{n}_a}, \underline{\mathbf{D}}^{a}_{\mathbf{n}_a}, \underline{\mathbf{K}}^{a}_{\mathbf{n}_a}$ are –abusively- named acoustic mass, damping and stiffness matrices and $\underline{\mathbf{C}}_{\mathbf{n}_s,\mathbf{n}_a}$ is the structural-acoustic coupling matrix. The underlining here indicates mean values.

For large size problems –many millions DOFS-, a modal reduction is usually performed. Vibration and acoustic response fields are respectively expressed using the *in vacuo* structural modes and the blocked-boundary acoustic modes. Associated so-called generalized coordinates, $\underline{\mathbf{q}}_{\Psi}{}^{s}(\omega), \underline{\mathbf{q}}_{\Phi}{}^{a}(\omega)$, are such that:

$$\begin{aligned} \underline{\mathbf{u}}^{s}(\omega) &= \underline{\boldsymbol{\Psi}} \underline{\mathbf{q}}_{\Psi}{}^{s}(\omega) \\ \underline{\mathbf{p}}^{a}(\omega) &= \underline{\boldsymbol{\Phi}} \underline{\mathbf{q}}_{\Phi}{}^{a}(\omega) \end{aligned} \tag{2}$$

Generalized coordinates verify the structural-acoustic system of equation, similar to (1), but after projection on the modal basis of the structure for the first line and projection on the modal basis of the cavity for the second line:

$$\begin{bmatrix} \underline{\mathbf{A}}^{s}_{\Psi}(\omega) & \underline{\mathbf{C}}_{\Psi,\Phi} \\ \omega^2 \underline{\mathbf{C}}_{\Psi,\Phi}{}^{\mathrm{T}} & \underline{\mathbf{A}}^{a}_{\Phi}(\omega) \end{bmatrix} \begin{bmatrix} \underline{\mathbf{q}}_{\Psi}{}^{s}(\omega) \\ \underline{\mathbf{q}}_{\Phi}{}^{a}(\omega) \end{bmatrix} = \begin{bmatrix} \underline{\mathbf{f}}_{\Psi}{}^{s}(\omega) \\ \underline{\mathbf{Q}}_{\Phi}{}^{a}(\omega) \end{bmatrix} \tag{3}$$

Where the reduced dynamic stiffness matrix of the structure, $\underline{\mathbf{A}}^{s}_{\Psi}(\omega)$, and the reduced admittance matrix of the cavity, $\underline{\mathbf{A}}^{a}_{\Phi}(\omega)$, keep similar expressions as above :

$$\underline{\mathbf{A}}^{s}_{\Psi}(\omega) = -\omega^2 \underline{\mathbf{M}}^{s}_{\Psi} + j\omega \underline{\mathbf{D}}^{s}_{\Psi} + \underline{\mathbf{K}}^{s}_{\Psi}$$

$$\underline{\mathbf{A}}^{a}_{\Phi}(\omega) = -\omega^2 \underline{\mathbf{M}}^{a}_{\Phi} + j\omega \underline{\mathbf{D}}^{a}_{\Phi} + \underline{\mathbf{K}}^{a}_{\Phi}$$

Modes properties ensure reduced mass and stiffness matrices are positives –or eventually semi-positive-diagonal matrices. Reduced damping matrices are most of the time full matrices.

The proposed stochastic modelling is based on a mathematical theory of random matrices (see [1] for further detail). Random realizations of the uncertain system can be constructed by mean of random matrices construction. Thus, mean matrices $\underline{\mathbf{M}}^{s}_{\Psi}, \underline{\mathbf{D}}^{s}_{\Psi}, \underline{\mathbf{K}}^{s}_{\Psi}, \underline{\mathbf{M}}^{a}_{\Phi}, \underline{\mathbf{D}}^{a}_{\Phi}, \underline{\mathbf{K}}^{a}_{\Phi}, \underline{\mathbf{C}}_{\Psi,\Phi}$ are replaced by random matrices $\mathbf{M}^{s}_{\Psi}, \mathbf{D}^{s}_{\Psi}, \mathbf{K}^{s}_{\Psi}, \mathbf{M}^{a}_{\Phi}, \mathbf{D}^{a}_{\Phi}, \mathbf{K}^{a}_{\Phi}, \mathbf{C}_{\Psi,\Phi}$ which are constructed using an algebraic method from the mean matrices for given dispersion parameters.

Equation (3) then becomes a stochastic equation:

$$\begin{bmatrix} \mathbf{A}^{s}_{\Psi}(\omega) & \mathbf{C}_{\Psi,\Phi} \\ \omega^2 \mathbf{C}_{\Psi,\Phi}{}^{\mathrm{T}} & \mathbf{A}^{a}_{\Phi}(\omega) \end{bmatrix} \begin{bmatrix} \mathbf{q}_{\Psi}{}^{s}(\omega) \\ \mathbf{q}_{\Phi}{}^{a}(\omega) \end{bmatrix} = \begin{bmatrix} \underline{\mathbf{f}}_{\Psi}{}^{s}(\omega) \\ \underline{\mathbf{Q}}_{\Phi}{}^{a}(\omega) \end{bmatrix} \tag{4}$$

Matrices involved in equation (4) are built using elementary random mass, stiffness, damping and coupling matrices in the same manner as (3). It is to be noted that when randomized, none of the matrices is diagonal anymore, when expressed in the functional basis of the eigen-modes of the mean model. Nevertheless, elementary matrices remain definite positive or definite semi-positive depending on the case.

Dispersion parameters have been identified such as the stochastic model totally includes actual measured values. The identification may be performed through a conventional minimization method or more likely invoking the maximum of likelihood principle. Indeed, the stochastic model provides probability density functions allowing the computing of the likelihood of any measured FRF.

Solutions of the stochastic problem are obtained by the means of a Monte-Carlo simulation, that is to say by solving a large number of independent realizations of system (4). The number of realizations required depends on the expected level of statistical achievement. The FRF's mean value and upper-bound (with .95 or .99 probability) converge within a few hundreds of realizations. Lower-bound requires more effort.

It is generally convenient to perform a quantile analysis [5], since it is the more general way to estimate probabilities when the density function is unknown. Using a higher number of realizations (many thousands), one may estimate the probability density function required for likelihood estimations.

2.2 Uncertain system modal analysis

In the previous section, we explained how to build a stochastic model from a FE model. We will describe here the physical content of this model. As far as any response of a linear dynamical system may be built from its eigen-modes, the analysis of the modes of the stochastic system provides a complete view on its behaviour.

For each realization of the stochastic model (featuring full matrices as explained previously), one can set-up the following stochastic eigen-value problem:

$$\left[-\Lambda \mathbf{M}_{\Psi}^{s} + \mathbf{K}_{\Psi}^{s}\right]\Psi = 0 \qquad (5)$$

Solutions of (5) for individual realizations of stiffness and mass matrices provide the stochastic modal basis $\{\boldsymbol{\Psi}\}_{\theta_j}$, where θ_j indicates the realization index.

As for experimental modal analysis, a modal shape similarity criterion is proposed. The Stochastic Modal Assurance Criterion (SMAC) is introduced between the mean mode i and stochastic mode j:

$$SMAC_{ij} = E\left\{\frac{\left\langle \underline{\boldsymbol{\Psi}}_{\mathbf{i}}, \boldsymbol{\Psi}_{\mathbf{j}}^{\theta_j} \right\rangle^2}{\left\langle \underline{\boldsymbol{\Psi}}_{\mathbf{i}}, \underline{\boldsymbol{\Psi}}_{\mathbf{i}} \right\rangle \left\langle \boldsymbol{\Psi}_{\mathbf{j}}^{\theta_j}, \boldsymbol{\Psi}_{\mathbf{j}}^{\theta_j} \right\rangle}\right\}_{\theta_j} \qquad (6)$$

where $E\{\ \}$ is the mathematical expectation.

Figure 2 shows the SMAC matrix between stochastic modes and mean modes of a car body, for the lower order modes. The matrix is mostly diagonal, showing minor effects of the uncertainty modelling on the modal shapes. One can then draw the frequency distribution of selected modes, identified by their similarity to a mean mode. Figure 3 and 4 show the distribution of uncertain frequencies of a car body global mode related to various uncertainities. The distribution associated to a dispersed mass matrix, with increasing dispersion parameter value (increasing dispersion amount) is plotted on figure 3. Figure 4 shows a similar plot for dispersed stiffness matrices, with increasing dispersion amount. As expected the distribution goes flat when the dispersion amount increases. It is remarkable that stiffness uncertainty lead to a lower shift of the modal frequency distribution's centre when increasing the dispersion amount. This result may be related to a well known practical fact: stiffness defects lower eigen-frequencies.

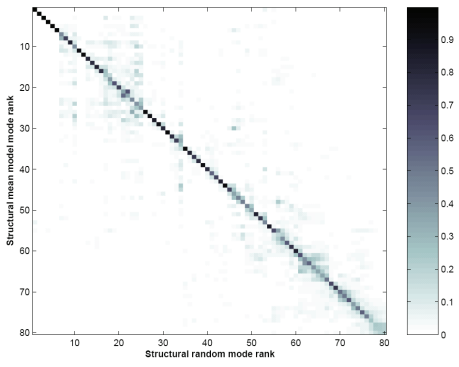

Figure 2: SMAC matrix between stochastic modes (x axis) and mean modes (y axis) -resulting of the proposed non-parametric method- for mode orders 1 to 80 of an uncertain car body

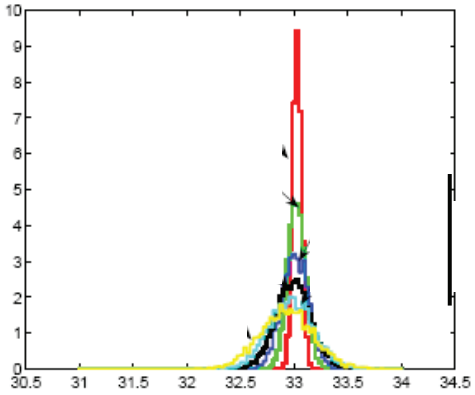

Figure 3: Torsion car body modal frequency distribution due to mass uncertainties. Ordered red, green, blue, black, cyan and yellow colours indicate increasing dispersion amount.

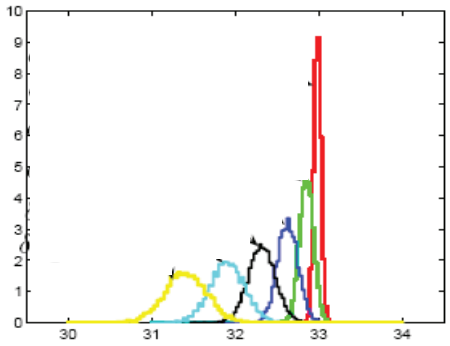

Figure 4: Torsion car body modal frequency distribution due to mass uncertainties. Ordered red, green, blue, black, cyan and yellow colours indicate increasing dispersion amount.

Figure 5 shows the SMAC matrix for higher order modes: uncertain modal shapes appear to be a combination of a range of mean mode shapes creating blurs around the diagonal. In this later case, it is difficult to recognize modal shapes and consequently to build statistics on the modal frequencies. This kind of behaviour could typically be related to mid frequencies where not only modal frequency disturbance occurs but also modal shape. Effect of this peculiar behaviour will later be mentioned.

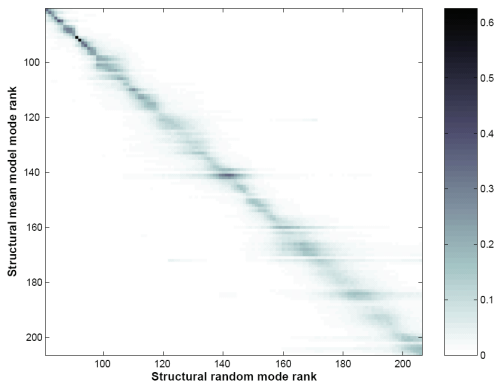

Figure 5: SMAC matrix between stochastic modes (x axis) and mean modes (y axis) -resulting of the proposed non-parametric method- for mode orders 80 to 200 of an uncertain car body

3 Energy density field model

Reference [6-7] details the construction of the proposed energy model from the realisations of a stochastic model, without any simplification in average. A similar approach was previously proposed in [8] in a deterministic and higher frequencies context, but already involving statistical issues since it was in the Frame work of the Statistical Energy Analysis.

This proposed model is derived from the general expression of the harmonic response of a vibro-acoustic system to random excitations:

$$\mathbf{S}_{RR} = \mathbf{T}\mathbf{S}_{EE}\mathbf{T}^{+}, \qquad (7)$$

Where $\mathbf{S}_{RR}$ is the cross-spectral vibro-acoustic response matrix, $\mathbf{S}_{EE}$ is the cross-spectral excitation matrix, $\mathbf{T}$ is the FRF matrix between observation and excitation points (obtained by solving equation (4) for every unitary excitations) and $^{+}$ indicate a conjugate and transposed matrix.

Every quantity used in this section and the following is –implicitly, when not mentioned- a function of frequency. Computations have to be repeated as many times as required to follow frequency responses.

In order to simplify explanations, only the structural case is presented here; response terms are structural velocities, while excitation terms are forces. Both are related by mobility matrices. In this case, expression (7) is re-written as:

$$\mathbf{S}_{VV} = \mathbf{T}\mathbf{S}_{FF}\mathbf{T}^{+} \qquad (7\text{bis})$$

where $\mathbf{S}_{VV}$ is the velocity response cross-spectral matrix, and $\mathbf{S}_{FF}$ is the force cross-spectral matrix.

In the case of an acoustic problem, response terms would be acoustic pressures and excitation terms would be acoustic flow velocity, both being related by admittance matrices.

3.1 Energy model construction

The proposed energy model simply relates the vector of input power on individual DOFs, $\boldsymbol{\pi}_{\mathbf{in}}$, to a response power along every observation DOF, $\boldsymbol{\pi}_{\mathbf{out}}$:

$$\boldsymbol{\pi}_{\mathbf{out}} = \boldsymbol{\xi}_{\mathbf{OI}}\boldsymbol{\pi}_{\mathbf{in}} \qquad (8)$$

where $\boldsymbol{\xi}_{\mathbf{OI}}$ is a positive, non-dimensional random Power Frequency Response Function (PFRF) matrix.

Let us introduce $\underline{\mathbf{Y}_{\mathbf{in}}}$ (*resp.* $\underline{\mathbf{Y}_{\mathbf{out}}}$) the stochastic average of the real part of the complex mobility matrix between all input points (*resp.* all observation points). These matrices -since they are real symmetric- may be decomposed as $\underline{\mathbf{Y}_{\mathbf{in}}} = \underline{\mathbf{X}_{\mathbf{in}}}\,\underline{\mathbf{Y}_{\mathbf{in}}^{\mathbf{diag}}}\,\underline{\mathbf{X}_{\mathbf{in}}^{+}}$ (resp. $\underline{\mathbf{Y}_{\mathbf{out}}} = \underline{\mathbf{X}_{\mathbf{out}}}\,\underline{\mathbf{Y}_{\mathbf{out}}^{\mathbf{diag}}}\,\underline{\mathbf{X}_{\mathbf{out}}^{+}}$) involving a diagonal positive matrix.

The decomposition reveals the principal mobility patterns thought the unitary matrices $\underline{\mathbf{X}_{\mathbf{in}}}$ (resp. $\underline{\mathbf{X}_{\mathbf{out}}}$), that define a new vector basis which components will be named patterns . Principal mobility patterns show the direction in which the vibro-acoustic response is collinear with the excitation pattern, that is to say no coupling exists between principal mobility patterns.

Whatever the excitation, it can be shown that one can write:

$$\boldsymbol{\pi}_{\mathbf{in}} = \underline{\mathbf{Y}_{\mathbf{in}}^{\mathbf{diag}}}\,\mathbf{s}_{\mathbf{F}_{\mathbf{in}}^{2}} \qquad (9)$$

where $\mathbf{s}_{F_{in}^2} = diag\left(\underline{\mathbf{X}_{in}}\mathbf{S}_{FF}\underline{\mathbf{X}_{in}^{+}}\right)$ is the vector of the Power Spectral Density (PSD) of the loads expressed in the basis of the input principal mobility.

One then introduces the non-dimensionnal symmetrical expression of the PFRF matrix:

$$\boldsymbol{\xi}_{OI} = \underline{\mathbf{Y}_{out}^{diag\ -1}}\mathbf{H}_{OI}\underline{\mathbf{Y}_{in}^{diag\ -1}} \qquad (10)$$

where $\mathbf{H}_{OI}$ is the term to term squared random transfer matrix expressed in the new input and output basis : $H_{OI,ij} = \left|T_{OI,ij}\right|^2$ et $\mathbf{T}_{OI} = \underline{\mathbf{X}_{out}}\mathbf{T}\underline{\mathbf{X}_{in}^{+}}$

Finally, the response power appears to be:

$$\boldsymbol{\pi}_{out} = \underline{\mathbf{Y}_{out}^{diag\ -1}}\mathbf{s}_{v_{out}^2} \qquad (11)$$

where $\mathbf{s}_{v_{out}^2} = diag\left(\underline{\mathbf{X}_{out}}\mathbf{S}_{VV}\underline{\mathbf{X}_{out}^{+}}\right)$ is the vector of the response velocity PSD expressed in the basis of output principal mobility.

Practically, this means that the PSD of vibro-acoustic responses may be obtained by computing successively:

- The input and output principal mobility basis
- The input power vector using (9)
- The response power vector using (10)
- The response velocity PSD vector, by inversion of expression (11)

As demonstrated in references [6-7] the stochastic average of the response PSD's expression (7) (diagonal terms of the response cross-spectral matrix) are computed exactly when using expressions (8), (9), (10), (11) instead of (7). It should be noted here that correlations between response patterns are lost when using the proposed approach which may cause some trouble in the case of radiation computations. Nevertheless the proposed energy-field model is valid for structural-acoustic problems, naturally including sound radiation issues in the structural-acoustic coupled formulation.

3.2 About the principal mobility basis

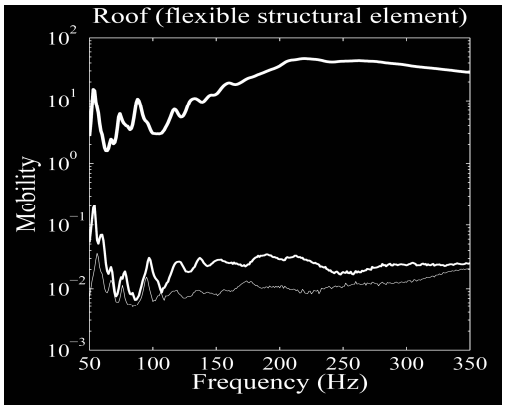

Figure 6: 3 principal mobility values vs frequency at one point on the roof (curved thin shell)

The use of the principal mobility basis is a critical point in the proposed energy approach. First, it validates the proposed expressions in any load case: indeed, expression (9) holds whatever the correlation

between forces coordinates in the input principal mobility basis. Relevant correlations between force excitations are implicitly accounted for when changing the basis.

Second, it separates -when needed- in-plane and normal displacements that are known to exhibit different dynamic properties. As an example figure 6 and 7 show respectively the principal mobilities computed for a point (3 DOFS) on the roof (Fig.6) and the right engine mount position (3 DOFs) on the right front side member (Fig. 7). On the roof (Fig.6) - slightly curved shell-, the normal direction shows a mobility that is many order of magnitude higher than in-plane mobility. On the front side member -curved beam with varying section-, the 3 principal mobilities have about the same order of magnitude.

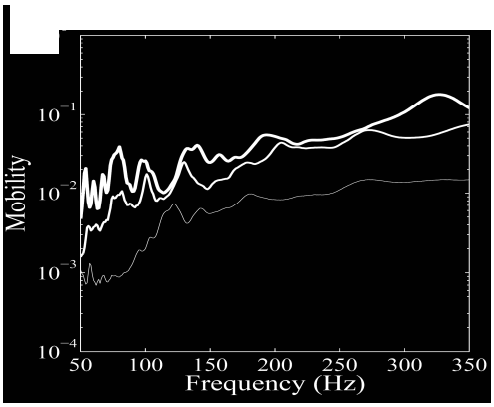

Figure 7: 3 principal mobility values vs frequency at one point on the front side member (curved beam)

The minimum extend of an input area is a single point with its 3 forces DOFS, as shown for figures 6 and 7. In this case, the principal mobility basis is obtained by a rotation of the axes providing a local axes system that is rather easy to work out.

When correlated forces are applied to multiple points, in a frequency range where strong distant interaction exist, the size of the relevant mobility matrix increases. Patterns associated to principal mobilities generally involve more than one input point, leading to a more complex excitation scheme. Such a physical scheme only occurs at low frequencies. When the frequency increases, both phenomena tend to disappear: cross-terms of input mobility matrices are vanishing, while distant forces tend –at least in average over a frequency band- to be uncorrelated.

In the following, we will only consider the principal mobility axes associated to one single point.

4 Simplified energy model and system partition

When compared to averaged FRFs, averaged PFRFs appear to be nearly frequency and location independent above a given frequency. Figure 8 (resp Figure 9) show 6 average FRF (resp PFRF) associated to 1 excitation DOF and 6 observations DOF on the roof, in the principal mobility direction (approximately the normal to the roof). Above 100 Hz, the 6 averaged PFRF merge to a single smooth frequency function, indicating the 6 considered DOF have the same response and could be described by a unique function associated to the whole area (e.g. the roof). A similar behaviour can be observed when comparing PFRF associated to many excitation DOFs in a limited area. It then seems possible to simplify the expression of the Power transfer between an excitation area and an observation area by replacing DOF to DOF PRFR by a single averaged PFRF. Such a simplification, when it is relevant, defines a partition of the studied system; excitation areas (later denoted *I*) may then be characterized by the overall power input, while observation areas (later denoted *O*) are characterized by a uniform response power. Only distant propagations are covered by the proposed simplification; local effects (excitation near-field) are out of scope of the proposed theory.

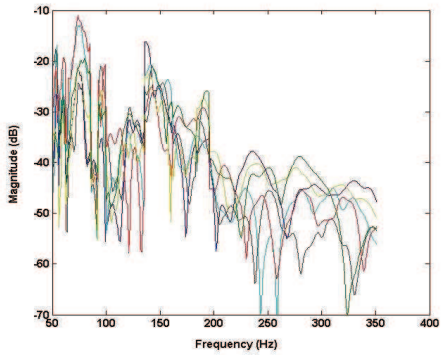

Figure 8: Averaged velocity FRFs between one excitation DOF (engine mount) and 6 observation DOF (maximum mobility direction) on the roof.

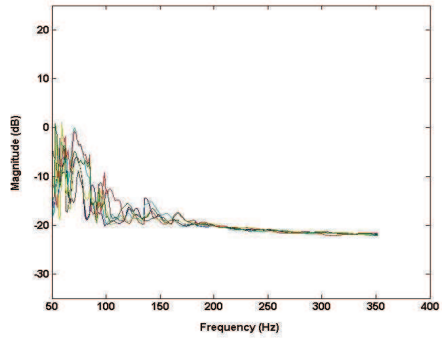

Figure 9: Averaged velocity PFRFs between one excitation DOF (engine mount) and 6 observation DOF (maximum mobility direction) on the roof.

One then introduces the scalar function e_{OI} -average PFRF-, which characterized the simplified distant power transmission, such as:

$$\Pi_{out} = e_{OI}\Pi_{in} \qquad (12)$$

where Π_{in} is the overall input power in the excitation area, $\Pi_{in} = \sum_{l=1}^{N_I} \pi_{in,k}$, and Π_{out} is the averaged response power in the observation area.

It can be shown that the best approximation –in a least square sense- is provided by the following expression:

$$e_{OI} = \frac{\sum_{l=1}^{N_I}\sum_{k=1}^{N_O} Y_{in,l}^{diag}\,\xi_{OI,lk}\,Y_{out,k}^{diag}}{\sum_{l=1}^{N_I} Y_{in,l}^{diag}\sum_{k=1}^{N_O} Y_{out,k}^{diag}} = \frac{\sum_{l=1}^{N_I}\sum_{k=1}^{N_O}\left|T_{OI,kl}\right|^2}{\sum_{l=1}^{N_I} Y_{in,l}^{diag}\sum_{k=1}^{N_O} Y_{out,k}^{diag}} \qquad (13)$$

The point to point error that is associated to the proposed simplification may be plotted as the matrix of differences between the true model and the simplified model:

$$\Delta_{OI,kl} = \left| Y_{out,k}^{diag}\xi_{k,l}Y_{in,l}^{diag} - Y_{out,k}^{diag}e_{OI}Y_{in,l}^{diag} \right| \qquad (14)$$

The root mean square difference is an indicator of the simplification (partition) relevance:

$$cmqe = \sqrt{\frac{1}{N_O N_I}\sum_{l=1}^{N_I}\sum_{k=1}^{N_O}\Delta_{OI,kl}^2} \qquad (15)$$

Figure 10 shows as an example the matrix $\mathbf{\Delta}_{OI}$ of the difference between the simplified model and the true model for four selected frequencies, in the case of PFRF between the car body front-end (30 excitation DOFs) and the interior cavity (12 DOFS). Figure 11 shows the associated root mean square difference (15) –plotted in dB- as a function of frequency. Above 100 Hz, the root mean square difference remains low, which indicates that the car body front-end and the cavity behave –within a limited error- as separated entities, related by a single PFRF.

It is noticeable that above 100 Hz, one may be sure that any decrease of the input power on the car front-end -whatever the way it comes- leads to a decrease of the response power, that is to say the acoustic pressure. In such a case, noise control inside the cavity just relies on the control of two frequency functions: the overall input power and the average PFRF. The sensitivity of both quantities to design parameters is discussed in a related paper [9].

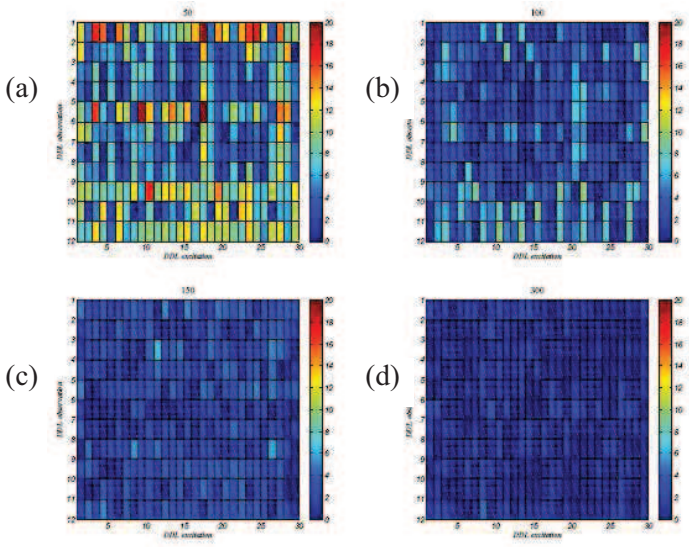

Figure 10: Matrix of differences (14) between the point to point PFRFs and the single averaged PFRF between the body front-end (30 DOFs) and the car interior cavity (12 DOFs). 50 Hz (a), 100 Hz (b), 150 Hz (c) and 300 Hz (d)

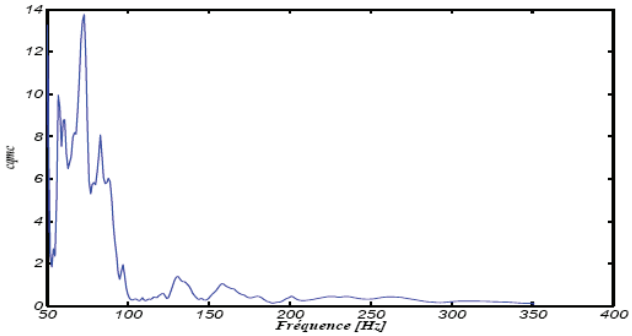

Figure 11: Root mean square difference (15) associated to the simplification of the PFRF between the body front-end (30 DOFs) and the car interior cavity (12 DOFs)

5 Conclusion

After a quick presentation of the non-parametric method used to investigate uncertain vibro-acoustic systems, an application to a car body modal analysis shows the main features of the proposed stochastic modelling in terms of modal shape and eventually modal frequencies. Modal shapes appear to be stable enough to perform frequencies statistics only at low frequencies.

An energy field density approach is then introduced. In the case of a complex, heterogeneous structure such as a car body, this stochastic approach reveals homogeneous behaviours with respect to space and frequency. Such behaviour appears for any load case, after a projection on the principal mobility basis of a given area (excitation or observation).

Above a given frequency, Power Frequency Response Functions between excitation DOFs within a given area and observation DOFs in a distant area, tend to merge to a unique scalar PFRF. A partition of the studied structure can than be created; it is such that one single averaged PFRF is enough to describe the power transfer between the parts constituted by the excitation and observation areas.

A specific measure is proposed to measure the relevance of the proposed simplification. It seems that in the case of an automotive structure, above 100 Hz, some parts already satisfy a partition condition. It is in particular the case of the car front-end and the cavity.

Such a scheme could be of great help to improve the noise control in automotive vehicle. It is reminded that the proposed scheme only holds in average in a stochastic context. The expected properties may not be fulfilled for individual realizations.

6 References

[1] Soize,C. *Random matrix theory for modelling random uncertainties in computational mechanics*, Comp. Meth. Appl. Mech. Eng. 194(12-16), 1333-1366. (2005)

[2] Soize, C. *A comprehensive overview of a non-parametric probabilistic approach of model uncertainties for predictive models in structural dynamics*, Journal of Sound and Vibration. 288(3), 623-652 (2005)

[3] Durand J.-F., Soize C., Gagliardini L. *Structural-acoustic modelling of automotive vehicles in presence of uncertainties and experimental identification and validation*, Journal of the Acoustical Society of America 24, 1513–1525 (2008)

[4] Ohayon, R., and Soize, C. *Structural Acoustics and Vibration*, Academic Press, San Diego. (1998)

[5] Serfling, R .J. *Approximation Theorems of Mathematical Statistics*, John Wiley & Sons. (1980)

[6] M. Kassem, C. Soize, L. Gagliardini, *Energy density field approach for low- and medium-frequency vibroacoustic analysis of complex structures using a statistical computational model*, Journal of Sound and Vibration, 323(3-5), 849-863 (2009).

[7] M. Kassem, C. Soize, L. Gagliardini, *Structural partitioning of complex structures in the medium-frequency range. An application to an automotive vehicle,* Journal of Sound and Vibration (Submitted on 7 February 2010).

[8] L. Gagliardini, G. Borello, *Virtual SEA: Towards an industrial process*, SAE International, 2007-01-2302, (2007).

[9] A. Jund, L. Gagliardini, *Noise control using input power at low and mid-frequencies: sensitivity to structural design changes,* ISMA conference, Leuven (2010)